IEEE Access
Multidisciplinary ⋮ Rapid Review ⋮ Open Access Journal

Received January 24, 2021, accepted February 14, 2021, date of publication February 16, 2021, date of current version March 1, 2021.
Digital Object Identifier 10.1109/ACCESS.2021.3059897

A Finite-Time Fault-Tolerant Control Using Non-Singular Fast Terminal Sliding Mode Control and Third-Order Sliding Mode Observer for Robotic Manipulators

VAN-CUONG NGUYEN, ANH-TUAN VO, AND HEE-JUN KANG
Department of Electrical, Electronic and Computer Engineering, University of Ulsan, Ulsan 44610, South Korea
Corresponding author: Hee-Jun Kang (hjkang@ulsan.ac.kr)

This research was supported by Basic Science Research Program through the National Research Foundation of Korea (NRF) funded by the Ministry of Education (2019R1D1A3A03103528).

ABSTRACT In this paper, a fault-tolerant control (FTC) method for robotic manipulators is proposed to deal with the lumped uncertainties and faults in case of lacking tachometer sensors in the system. First, the third-order sliding mode (TOSM) observer is performed to approximate system velocities and the lumped uncertainties and faults. This observer provides estimation information with high precision, low chattering phenomenon, and finite-time convergence. Then, an FTC method is proposed based on a non-singular fast terminal switching function and the TOSM observer. This combination provides robust features in dealing with the lumped uncertainties and faults, increases the control performance, reduces chattering phenomenon, and guarantees fast finite-time convergence. Especially, this paper considers both two periods of time, in which before and after the convergence process takes place. The stability and the finite-time convergence of the proposed controller-observer technique is demonstrated using the Lyapunov theory. Finally, to verify the effectiveness of the proposed controller-observer technique, computer simulation on a serial two-link robotic manipulator is performed.

INDEX TERMS Fault-tolerant control, controller-observer strategy, third-order sliding mode observer, non-singular fast terminal sliding mode control, robotic manipulators.

I. INTRODUCTION

In the industrial environment, robotic manipulators have many special applications due to their ability to replace workers in difficult and dangerous activities such as moving heavy products, assembling mechanical structures, sheet metal cutting, etc. Moreover, they can help to improve both the product quality and quantity, thus saving the cost for manufacturers. However, robotic manipulators have very complicated dynamic, from practical viewpoint, they are arduous or even impossible to obtain the robot's exact dynamics, leading to model uncertainties. They are the large challenges in both theoretical and practical control. In addition, along with modern industrial applications becoming increasingly complex, faults more frequently happen in the system especially in the condition of long-term operation. Hence, the requirement is to be able to automatically detect the faults, compensates their effects, and completes the assigned missions even in the existence of one or more faults with acceptable performance. In literature, various methods have been proposed to handle the effects of the uncertainties and faults. In some papers, the system uncertainties and faults are approximated separately [1]–[4]. However, using two separate observers makes the algorithms cumbersome that leads to resources and time consuming for computation. In this paper, the faults are treated as additional uncertainties, thus, the total effects of the lumped uncertainties and faults in the system are considered.

In order to deal with the lumped uncertainties and faults, fault-tolerant control (FTC) methods have been developed [5], [6]. In general, the FTC tactics can be divided into two categories: passive FTC (PFTC) [7], [8] and active FTC (AFTC) [9], [10]. In PFTC technique, a robust controller is designed to compensate the faults without requiring

The associate editor coordinating the review of this manuscript and approving it for publication was Mohammad Alshabi.

information feedback from a fault diagnosis observer. Since the faults' effects imposed on the nominal controller of the PFTC are heavier than that of the AFTC, the nominal controller of the PFTC requires stronger robustness against the effects of faults. On the other hand, an AFTC is constructed based on online fault diagnosis technologies. Compared with the PFTC, the AFTC accommodates higher control performance when the fault information is approximated correctly. Therefore, the AFTC methods are more suitable for practical applications.

In literature, various control approaches have been developed for FTC, such as computed torque control [1], [11], adaptive control [12], [13], neural network control [14], [15], fuzzy logic control [16]–[18], and sliding mode control (SMC) [19]–[26], etc. Compared with others, SMC stands out with superior control properties like fast convergence, high tracking precision, and robustness against the lumped uncertainties and faults. In addition, it is pretty simple in design; therefore, the SMC has been extensively employed to control robotic manipulator system in literature. Besides the huge advantages, there still exists some big limitations that degrade the practical applicability of the conventional SMC, that are: 1) the finite-time convergence cannot be guaranteed, 2) chattering phenomenon, 3) velocity (and acceleration) measurements are required.

To overcome the first limitation – the finite-time convergence, the terminal SMC (TSMC) has been developed by utilizing nonlinear switching functions instead of the linear one [27], [28]. In addition, it can reach higher exactness by rigorously selecting parameters. The conventional TSMC, however, produces two major drawbacks, that are singularity problem and slower dynamic response compared with the conventional SMC. To overcome these limitations, the fast TSMC (FTSMC) [29], [30] and the non-singular TSMC (NTSMC) [31], [32] have been proposed. However, they can only handle each problem separately. In order to resolve the two problems at the same time, the non-singular fast TSMC (NFTSMC) has been investigated. In addition, the NFTSMC has the capability to obtain high tracking error precision and provide feature robustness against the influence of the lumped uncertainties and faults; therefore, this control algorithm has been extensively utilized by many researchers [33]–[36]. Unfortunately, the last two limitations still remain.

To eliminate the second limitation – chattering phenomenon, which is caused by the utilizing of a discontinuous term with a big and fixed gain in reaching phase, the basic idea is to use an observer to approximate the lumped uncertainties and faults and then compensates its effects in the system. By using this method, the switching gain is now chosen smaller to deal with the effects of the estimation error instead of the effects of the lumped uncertainties and faults; thus, the chattering phenomenon is reduced. In the literature, many researchers have been paid attention to develop an effective observer to approximate the lumped uncertainties and faults such as [34], [37]–[47]. With the learning ability and high accuracy estimation, the neural network (NN) observer has been widely employed [41]–[43]. On the other hand, the learning ability makes the system more complicated and thus requires higher system configuration to use online training technique that increases the cost of devices. The time delay estimation (TDE) method, in [34], [44], [45], is a simpler technique; however, it needs the velocity measurement that not usually available in practical. The sliding mode observer, especially, the third-order sliding mode (TOSM) observer, in [46], has ability to estimate the lumped uncertainties and faults with high accuracy and less chattering. Moreover, the TOSM observer provides the system velocity (and acceleration) estimation with finite-time convergence. Therefore, the third limitation of the SMC is eliminated. Thanks to the above advantages, the TOSM observer has been broadly utilized in controlling theory [39], [40], [47].

In this paper, the TOSM observer is used to approximate the velocities and the lumped uncertainties and faults of robotic manipulator system. The obtained velocities are employed in the system to replace the measured velocity and the estimated uncertainties and faults are applied to reduce their effects. To achieve high position tracking precision and stability of the system, a robust control is design based on a terminal sliding function. Especially, two periods of time that before and after the convergence process takes place, are carefully considered. The proposed FTC strategy affords high tracking accuracy, low chattering phenomenon, non-singularity, robustness against the effects of the lumped uncertainties and faults, and finite-time convergence for both position tracking errors and velocity estimation.

In this paper, the FTC method that combines the NFTSMC and the TOSM observer is proposed for the robotic manipulator system to surpass the total effects of the lumped uncertainties and faults. The main contributions of this paper are given as following:

(1) Proposing an NFTSM switching function based on estimated state from TOSM observer,

(2) Proposing an FTC method to enhance the tracking performance of the robotic system under the total effect of the lumped uncertainties and faults,

(3) Reducing the chattering phenomenon in control input signals by estimating and compensating the lumped uncertainties and faults,

(4) Demonstrating the finite-time stability of the switching function and the robotic system using the Lyapunov stability theory,

(5) Eliminating the necessary of system velocity measurement in the design procedure,

(6) Considering both two periods of time, in which before and after the convergence process takes place.

This paper is structured into six parts. Next to the introduction, the problem statement is presented in Section II. Then, the TOSM observer is designed for the robotic manipulator systems in Section III. Section IV presents the design of the FTC algorithm using the NFTSMC and the TOSM observer. In Section V, computer simulations on a serial two-link robotic manipulator are presented to demonstrate the effectiveness of the proposed controller-observer algorithm. Finally, Section VI gives some conclusions.

II. PROBLEM STATEMENT

A. SYSTEM IN NORMAL OPERATION CONDITION

Consider a serial n-link robotic manipulator in normal operation condition with the dynamic equation as

$$M(\theta)\ddot{\theta} + C(\theta, \dot{\theta}) + G(\theta) + F(\dot{\theta}) + \tau_d(t) = \tau(t) \quad (1)$$

where $\theta, \dot{\theta}, \ddot{\theta} \in \Re^n$ represent position, velocity, and acceleration of robot joints, respectively. $M(\theta) \in \Re^{n\times n}$, $C(\theta, \dot{\theta}) \in \Re^n$, and $G(\theta) \in \Re^n$ denote the inertia matrix, the Coriolis and centripetal forces, and the gravitational force term, respectively. $F(\dot{\theta}) \in \Re^n$ is the friction vector, $\tau(t) \in \Re^n$ denotes the control input torque, and $\tau_d(t) \in \Re^n$ represents the disturbance vector.

In realization, since the difference between the mathematical and practical model, the model functions of the robotic manipulator can be expressed as

$$M(\theta) = M_0(\theta) + \Delta M(\theta) \quad (2)$$

$$C(\theta, \dot{\theta}) = C_0(\theta, \dot{\theta}) + \Delta C(\theta, \dot{\theta}) \quad (3)$$

$$G(\theta) = G_0(\theta) + \Delta G(\theta) \quad (4)$$

where $M_0(\theta)$, $C_0(\theta, \dot{\theta})$, and $G_0(\theta)$ represent the nominal model; the terms $\Delta M(\theta)$, $\Delta C(\theta, \dot{\theta})$, and $\Delta G(\theta)$ are the unmodeled components.

Thus, we can rewrite the robot dynamic equation (1) as

$$M_0(\theta)\ddot{\theta} + C_0(\theta, \dot{\theta}) + G_0(\theta) = \tau(t) + \Theta(\theta, \dot{\theta}, t) \quad (5)$$

where $\Theta(\theta, \dot{\theta}, t) = -\Delta M(\theta) - \Delta C(\theta, \dot{\theta}) - \Delta G(\theta) - F(\dot{\theta}) - \tau_d(t)$ denotes the uncertainties of the robot system.

The equation (5) can be transformed to the below form

$$\ddot{\theta} = \Upsilon(\theta, \dot{\theta}, t) + M_0^{-1}(\theta)\tau(t) + \Pi(\theta, \dot{\theta}, t) \quad (6)$$

where $\Pi(\theta, \dot{\theta}, t) = M_0^{-1}(\theta)\Theta(\theta, \dot{\theta}, t)$ represents the uncertainty terms of the robotic system and $\Upsilon(\theta, \dot{\theta}, t) = M_0^{-1}(\theta)\left[-C_0(\theta, \dot{\theta}) - G_0(\theta)\right]$ represents the nominal function of the robotic system.

B. SYSTEM IN FAULT AFFECTED OPERATION CONDITION

Nowadays, with modern industrial applications becoming increasingly complex, faults more frequently happen in a system especially in the condition of long-term operation. Therefore, in this paper, we assume that the robot system works under the effect of faults. Thus, the robot dynamic (6) becomes

$$\ddot{\theta} = \Upsilon(\theta, \dot{\theta}, t) + M_0^{-1}(\theta)\tau(t) + \Pi(\theta, \dot{\theta}, t) + \Psi(\theta, \dot{\theta}, t) \quad (7)$$

where $\Psi(\theta, \dot{\theta}, t) = \xi(t - T_f)\Phi(\theta, \dot{\theta}, t)$ represents the unknown but bounded faults that happen at time T_f. The term $\xi(t - T_f) = diag\{\xi_1(t - T_f), \xi_2(t - T_f), \ldots, \xi_n(t - T_f)\}$ represents the time profile of the unknown faults, in which

$$\xi_i(t - T_f) = \begin{cases} 0 & if\ t \le T_f \\ 1 - e^{-\zeta_i(t - T_f)} & if\ t \ge T_f \end{cases}$$

with $\zeta_i > 0$ represent the evolution rate, $(i = 1, 2, \ldots, n)$.

Remark 1: In robotic manipulator systems, faults can be actuator faults, sensor faults, and process faults. However, this paper focus to solve the system with actuator faults. Therefore, the fault functions $\Phi(\theta, \dot{\theta}, t)$ are defined as faults which occur in the actuator.

In this paper, the unknown faults will be treated as additional uncertainties, thus we consider the total effect of the lumped uncertainties and faults in the system.

By defining $x_1 = \theta, x_2 = \dot{\theta}, x = \left[x_1^T\ x_2^T\right]^T$, we transfer the robot dynamic (7) into the state space form as

$$\begin{aligned} \dot{x}_1 &= x_2 \\ \dot{x}_2 &= \Upsilon(x, t) + M_0^{-1}(x_1)\tau(t) + D(x, t) \end{aligned} \quad (8)$$

where $D(x, t) = \Pi(x, t) + \Psi(x, t)$ represents the lumped uncertainties and faults.

The main objective of this paper is to design a controller-observer strategy that deals with the effects of the lumped uncertainties and faults and achieve minimum tracking errors. The proposed controller-observer method is designed based on the assumptions as following:

Assumption 1: The lumped uncertainties and faults $_D(x, t)$ are bounded as

$$|D(x, t)| \le \Delta_D \quad (9)$$

where Δ_D is a known positive constant.

Assumption 2: There exists the time derivative of the lumped uncertainties and faults and they are bounded as

$$\left|\frac{d}{dt}D(x, t)\right| \le \Delta_{\dot{D}} \quad (10)$$

where $\Delta_{\dot{D}}$ is a known positive constant. Note that the assumption 2 is realistic and was used in many papers [48]–[50].

III. DESIGN OF THE THIRD-ODER SLIDING MODE OBSERVER

In this section, the TOSM observer is designed to approximate the system velocities, which is assumed unavailable because of the lacking tachometer sensors in the system. In addition, the lumped uncertainties and faults will be reconstructed from the estimated signal and then employed to design the control in the next section.

A. DESIGN OF THE OBSERVER

The TOSM observer is designed for the robotic system (8) as [23]

$$\begin{aligned} \dot{\hat{x}}_1 &= \gamma_1 |x_1 - \hat{x}_1|^{2/3}\ sign(\tilde{x}_1) + \hat{x}_2 \\ \dot{\hat{x}}_2 &= \Upsilon(\hat{x}, t) + M_0^{-1}(x_1)\tau(t) \\ &\quad + \gamma_2 |x_1 - \hat{x}_1|^{1/3}\ sign(x_1 - \hat{x}_1) - \hat{z} \end{aligned}$$

$$\dot{\hat{z}} = -\gamma_3 \, sign\left(x_1 - \hat{x}_1\right) \tag{11}$$

where $\hat{x}$ is the estimator of the true state x, and γ_i represent the observer gains, $(i = 1, 2, 3)$.

By subtracting (11) from (8), we can obtain

$$\begin{aligned} \dot{\tilde{x}}_1 &= -\gamma_1 \left|\tilde{x}_1\right|^{2/3} sign\left(\tilde{x}_1\right) + \tilde{x}_2 \\ \dot{\tilde{x}}_2 &= -\gamma_2 \left|\tilde{x}_1\right|^{1/3} sign\left(\tilde{x}_1\right) + D(x,t) - d\left(\tilde{x},t\right) + \hat{z} \\ \dot{\hat{z}} &= -\gamma_3 \, sign\left(\tilde{x}_1\right) \end{aligned} \tag{12}$$

where $\tilde{x} = x - \hat{x}$ represent the state estimation errors and $d\left(\tilde{x},t\right) = \left[\Upsilon\left(\hat{x},t\right) + M_0^{-1}\left(x_1\right)\tau\right] - \left[\Upsilon\left(x,t\right) + M_0^{-1}\left(x_1\right)\tau\right]$. We assume that the term $d\left(\tilde{x},\tau,t\right)$ and its derivative are bounded as $\left|d\left(\tilde{x},t\right)\right| \leq \Delta_d$ and $\left|\dot{d}\left(\tilde{x},t\right)\right| \leq \Delta_{\dot{d}}$.

The estimation errors (12) can be rewritten as follow

$$\begin{aligned} \dot{\tilde{x}}_1 &= -\gamma_1 \left|\tilde{x}_1\right|^{2/3} sign\left(\tilde{x}_1\right) + \tilde{x}_2 \\ \dot{\tilde{x}}_2 &= -\gamma_2 \left|\tilde{x}_1\right|^{1/3} sign\left(\tilde{x}_1\right) + \hat{z}_0 \\ \dot{\hat{z}}_0 &= -\gamma_3 \, sign\left(\tilde{x}_1\right) + \dot{\hat{\Delta}}\left(x,t\right) \end{aligned} \tag{13}$$

where $\hat{z}_0 = \hat{D}\left(x,t\right) + \hat{z}$ with $\hat{D}\left(x,t\right) = D\left(x,t\right) - d\left(\tilde{x},t\right)$.

The error dynamic (13) is in the standard form of robust exact second-order differentiator; according to [51], the stable and finite-time convergence of the differentiator has completely demonstrated. The observer gains can be selected as $\gamma_1 = \alpha_1 L^{1/3}$, $\gamma_2 = \alpha_2 L^{2/3}$, and $\gamma_3 = \alpha_3 L$ where $\alpha_1 = 2$, $\alpha_2 = 2.12$, $\alpha_3 = 1.1$, and $L = \Delta_{\dot{D}} + \Delta_{\dot{d}}$.

B. UNCERTAINTIES AND FAULTS RECONSTRUCTION

After the convergence time, the estimated states ($\hat{x}_1$, and $\hat{x}_2$) will reach the true states (x_1, and x_2), respectively. The estimation errors (13) becomes

$$\begin{aligned} \dot{\tilde{x}}_1 &= -\gamma_1 \left|\tilde{x}_1\right|^{2/3} sign\left(\tilde{x}_1\right) + \tilde{x}_2 \equiv 0 \\ \dot{\tilde{x}}_2 &= -\gamma_2 \left|\tilde{x}_1\right|^{1/3} sign\left(\tilde{x}_1\right) + \hat{z}_0 \equiv 0 \\ \dot{\hat{z}}_0 &= -\gamma_3 \, sign\left(\tilde{x}_1\right) + \dot{\hat{\Delta}}\left(x,t\right) \equiv 0 \end{aligned} \tag{14}$$

As a result, the estimation errors of the lumped uncertainties and faults, $d\left(\tilde{x},t\right)$, will become zero; therefore, the estimation of the lumped uncertainties and faults are reconstructed as

$$\hat{D}\left(x,t\right) = \int \gamma_3 \, sign\left(\tilde{x}_1\right) \tag{15}$$

As we can see in (15), the obtained signal consists of an integral operator; hence, the estimation information of the TOSM observer can be reconstructed directly without filtration. Consequently, this observer provides estimation signal with higher accuracy and low chattering than that of SOSM observer [52]. This estimation information will be performed to design the FTC method in the next section.

Remark 2: Even if in the ideal sliding motion, we can only to get the exact estimation information after the convergence process. When employing the obtained estimation to the system, the estimation errors which appear in transient time will affect the selecting parameters of the controller. If we do not consider these components strictly, it will cause incorrect in selection of control parameters and thus affect the system stability.

IV. CONTROLLER DESIGN

In this section, an FTC method using NFTSMC is designed to handle the effects of the lumped uncertainties and faults with low chattering phenomenon and high tracking performance. Especially, the control technique is designed based on the assumption that only the tachometer sensors are unavailable in the robotic system. The analysing process is divided into two periods as following.

A. DESIGN OF NFTSM SWITCHING FUNCTION

The tracking errors and velocity errors are defined as following

$$e = x_1 - x_d \tag{16}$$

$$\dot{\hat{e}} = \hat{x}_2 - \dot{x}_d \tag{17}$$

where x_d, $\dot{x}_d$ represent the desired trajectories and velocities, respectively.

In order to design the control input, an NFTSM switching function based on TOSM observer is chosen as the following expression

$$\hat{s} = \dot{\hat{e}} + \frac{2\kappa_1}{1+\exp(-\mu_1(|e|-\phi))} e + \frac{2\kappa_2}{1+\exp(\mu_2(|e|-\phi))} |e|^{\alpha} \, sign\left(e\right) \tag{18}$$

where κ_1, κ_2, μ_1, μ_2 are positive constants, $0 < \alpha < 1$ and $\phi = \left(\frac{\gamma_2}{\gamma_1}\right)^{1/(1-\alpha)}$.

Based on the SMC theory, when the system operates in the sliding mode, the following constraints are satisfied:

$$\begin{aligned} \hat{s} &= 0 \\ \dot{\hat{s}} &= 0 \end{aligned} \tag{19}$$

Therefore, the sliding mode dynamics can be obtained as

$$\dot{\hat{e}} = -\frac{2\kappa_1}{1+\exp(-\mu_1(|e|-\phi))} e - \frac{2\kappa_2}{1+\exp(\mu_2(|e|-\phi))} |e|^{\alpha} \, sign\left(e\right) \tag{20}$$

Theorem 1: For the sliding mode dynamics (20), the origin, e, is defined as the stable equilibrium point and the state trajectories of the dynamic system (20) converge to zero in the finite-time.

Proof: We can acquire the time derivative of the tracking errors (16) as

$$\begin{aligned} \dot{e} &= \dot{x}_1 - \dot{x}_d \\ &= x_2 - \dot{x}_d \end{aligned} \tag{21}$$

According to the definition of the estimation errors in part III, the velocity errors (17) can be rewritten as

$$\begin{aligned} \dot{\hat{e}} &= \hat{x}_2 - \dot{x}_d \\ &= x_2 - \dot{x}_d - \tilde{x}_2 \end{aligned} \tag{22}$$

After the convergence estimation errors, the estimated states, $\hat{x}_2$, will reach the true states, x_2. Therefore, the velocity errors (22) become

$$\hat{\dot{e}} = x_2 - \dot{x}_d = \dot{e} \tag{23}$$

Consider the Lyapunov function candidate as

$$V_1 = \frac{1}{2}e^2 \tag{24}$$

Differentiating the Lyapunov function (24) with respect to time and substituting the result from (20), we obtain

$$\begin{aligned} \dot{V}_1 &= e\dot{e} \\ &= -\frac{2\kappa_1}{1+\exp(-\mu_1(|e|-\phi))}e^2 \\ &\quad -\frac{2\kappa_2}{1+\exp(\mu_2(|e|-\phi))}|e|^{\alpha+1} \\ &< 0 \end{aligned} \tag{25}$$

It is shown that $V_1 > 0$ and $\dot{V}_1 < 0$, hence, the origin, e, of the sliding mode dynamic (20) is stable and the state trajectories e and $\dot{e}$ converge to zero in the finite-time. Consequently, the tracking velocity errors $\hat{\dot{e}}$ converge to zero in the finite-time. Therefore, the theorem 1 is completely demonstrated.

B. DESIGN OF FTC METHOD

1) BEFORE THE CONVERGENCE TIME

To achieve the control objective for the robotic system (8), a controller-observer technique is described in Theorem 2.

Theorem 2: For the robotic manipulator system (8), if the control input signal is designed as (26-28), then the system is stable, and the tracking error converges to zero in finite time.

The control law is designed as below

$$\tau = -M_0(x_1)\left(\tau_{eq} + \tau_{sw}\right) \tag{26}$$

with the equivalent control law, τ_{eq}, and the switching control law, τ_{sw}, are designed as following

$$\begin{aligned} \tau_{eq} &= -\ddot{x}_d + \Upsilon(x,t) + \gamma_2 |\tilde{x}_1|^{1/3}\ sign(\tilde{x}_1) + \int \gamma_3\ sign(\tilde{x}_1) \\ &\quad + \hat{\dot{e}} \left[\begin{array}{l} \frac{2\kappa_1}{1+\exp(-\mu_1(|e|-\phi))} \\ \quad + \frac{2\kappa_1\mu_1 sign(e)\exp(-\mu_1(|e|-\phi))}{[1+\exp(-\mu_1(|e|-\phi))]^2} \\ + \frac{2\kappa_2\alpha}{1+\exp(\mu_2(|e|-\phi))}|e|^{\alpha-1} \\ \quad - \frac{2\kappa_2\mu_2\exp(\mu_2(|e|-\phi))}{[1+\exp(\mu_2(|e|-\phi))]^2}|e|^{\alpha} \end{array} \right] \end{aligned} \tag{27}$$

$$\tau_{sw} = (\Delta_d + \mu)\ sign(\hat{s}) \tag{28}$$

where μ is a small positive constant.

Proof: We can acquire the time derivative of the switching function (18) as

$$\begin{aligned} \dot{\hat{s}} &= \frac{d}{dt}\hat{\dot{e}} \\ &\quad + \hat{\dot{e}} \left[\begin{array}{l} \frac{2\kappa_1}{1+\exp(-\mu_1(|e|-\phi))} + \frac{2\kappa_1\mu_1 sign(e)\exp(-\mu_1(|e|-\phi))}{[1+\exp(-\mu_1(|e|-\phi))]^2} \\ + \frac{2\kappa_2\alpha}{1+\exp(\mu_2(|e|-\phi))}|e|^{\alpha-1} - \frac{2\kappa_2\mu_2\exp(\mu_2(|e|-\phi))}{[1+\exp(\mu_2(|e|-\phi))]^2}|e|^{\alpha} \end{array} \right] \end{aligned} \tag{29}$$

Taking the time derivative of velocity errors and substituting the second equation of the TOSM observer (11) yields

$$\begin{aligned} \frac{d}{dt}\hat{\dot{e}} &= \dot{\hat{x}}_2 - \ddot{x}_d \\ &= -\ddot{x}_d + \Upsilon(\hat{x},t) + M_0^{-1}(x_1)\tau \\ &\quad + \gamma_2|\tilde{x}_1|^{1/3}\ sign(\tilde{x}_1) + \int \gamma_3\ sign(\tilde{x}_1) \\ &= -\ddot{x}_d + \Upsilon(x,t) + M_0^{-1}(x_1)\tau + d(\tilde{x},t) \\ &\quad + \gamma_2|\tilde{x}_1|^{1/3}\ sign(\tilde{x}_1) + \int \gamma_3\ sign(\tilde{x}_1) \end{aligned} \tag{30}$$

Substituting (29) into (30) yields

$$\begin{aligned} \dot{\hat{s}} &= -\ddot{x}_d + \Upsilon(x,t) + M_0^{-1}(x_1)\tau + d(\tilde{x},t) \\ &\quad + \gamma_2|\tilde{x}_1|^{1/3}\ sign(\tilde{x}_1) + \int \gamma_3\ sign(\tilde{x}_1) \\ &\quad + \hat{\dot{e}} \left[\begin{array}{l} \frac{2\kappa_1}{1+\exp(-\mu_1(|e|-\phi))} + \frac{2\kappa_1\mu_1 sign(e)\exp(-\mu_1(|e|-\phi))}{[1+\exp(-\mu_1(|e|-\phi))]^2} \\ + \frac{2\kappa_2\alpha}{1+\exp(\mu_2(|e|-\phi))}|e|^{\alpha-1} - \frac{2\kappa_2\mu_2\exp(\mu_2(|e|-\phi))}{[1+\exp(\mu_2(|e|-\phi))]^2}|e|^{\alpha} \end{array} \right] \end{aligned} \tag{31}$$

Employing the control input (26-28) into (31), we achieve

$$\dot{\hat{s}} = -(\Delta_d + \mu)\ sign(\hat{s}) + d(\tilde{x},t) \tag{32}$$

Consider the Lyapunov function candidate as

$$V_2 = \frac{1}{2}\hat{s}^T\hat{s} \tag{33}$$

Differentiating the Lyapunov function (33) with respect to time and substituting the result from (32), we obtain

$$\begin{aligned} \dot{V}_2 &= \hat{s}^T\dot{\hat{s}} \\ &= \hat{s}^T\left(-(\Delta_d+\mu)\ sign(\hat{s}) + d(\tilde{x},t)\right) \\ &= -(\Delta_d+\mu)\sum_{i=1}^{n}|\hat{s}_i| + d(\tilde{x},t)^T\hat{s} \le -\mu\sum_{i=1}^{n}|\hat{s}_i| \\ &\le -\mu\|\hat{s}\| = -\sqrt{2}\mu V_2^{1/2} < 0, \quad \forall \hat{s} \ne 0 \end{aligned} \tag{34}$$

According to the stability theory in [53], it can be concluded that the robotic system (8) is stable and the tracking error converges to zero after finite time. Thus, the Theorem 2 is completely demonstrated.

2) AFTER THE CONVERGENCE TIME

In this part, we consider the control law after the convergence process. After the convergence time, the term $\gamma_2|\tilde{x}_1|^{1/3}\ sign(\tilde{x}_1)$ in the equivalent control law (27) converts to zero; therefore, the control law (26-28) will become

$$\tau = -M_0(x_1)\left(\tau_{eq} + \tau_{sw}\right) \tag{35}$$

$$\begin{aligned} \tau_{eq} &= -\ddot{x}_d + \Upsilon(x,t) + \int \gamma_3\ sign(\tilde{x}_1) \\ &\quad + \hat{\dot{e}} \left[\begin{array}{l} \frac{2\kappa_1}{1+\exp(-\mu_1(|e|-\phi))} \\ \quad + \frac{2\kappa_1\mu_1 sign(e)\exp(-\mu_1(|e|-\phi))}{[1+\exp(-\mu_1(|e|-\phi))]^2} \\ \quad + \frac{2\kappa_2\alpha}{1+\exp(\mu_2(|e|-\phi))}|e|^{\alpha-1} \\ \quad - \frac{2\kappa_2\mu_2\exp(\mu_2(|e|-\phi))}{[1+\exp(\mu_2(|e|-\phi))]^2}|e|^{\alpha} \end{array} \right] \end{aligned} \tag{36}$$

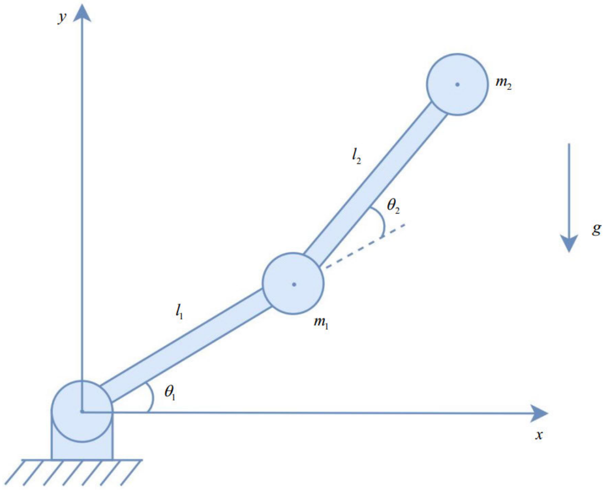

FIGURE 1. Two-link robotic manipulator.

$$\tau_{sw} = (\Delta_d + \mu)\, sign\left(\hat{s}\right) \tag{37}$$

Generally, the control law in (35-37) is employed to the system; however, the missing of the component $\gamma_2 \left|\tilde{x}_1\right|^{1/3} sign\left(\tilde{x}_1\right)$ leads to incorrect in selecting parameters and may affect the operation of the system at the initial stage and when faults happen. Therefore, this paper performs the control law in (26-28) instead of the control law in (35-37).

The proposed controller-observer technique provides some superior control properties such as high tracking control precision with finite-time convergence, faster dynamic response, low chattering phenomenon, non-singularity, velocity measurement elimination and robustness against the lumped uncertainties and faults. Its efficiency will be demonstrated in the simulation part.

V. NUMERICAL SIMULATIONS

To demonstrate the effectiveness of the proposed FTC technique, computer simulations are performed on a serial two-link robotic manipulator which is presented in Fig.1. The detailed dynamic model of the two-link robot is given as following

Inertia term

$$M(\theta) = \begin{bmatrix} M_{11} & M_{12} \\ M_{21} & M_{22} \end{bmatrix}$$

where

$$\begin{aligned} M_{11} &= m_1 l_{c1}^2 + m_2(l_1^2 + l_{c2}^2 + 2l_1 l_{c2} cos(\theta)) + I_1 + I_2 \\ M_{12} &= M_{21} = m_1 l_{c2}^2 + m_2 l_{c2} l_1 cos(\theta) + I_2 \\ M_{22} &= m_2 l_{c2}^2 + I_2 \end{aligned}$$

Coriolis and centripetal term

$$C(\theta, \dot{\theta}) = \begin{bmatrix} -2m_2 l_1 l_{c2}\, sin(\theta)\dot{\theta}_1\dot{\theta}_2 - m_2 l_1 l_{c2}\, sin(\theta_2)\dot{\theta}_2^2 \\ m_2 l_1 l_{c2}\, sin(\theta_2)\dot{\theta}_1^2 \end{bmatrix}$$

Gravitational term

$$G(\theta) = \begin{bmatrix} m_1 g l_{c1}\cos(\theta_1) + m_2 g\left(l_1\cos(\theta_1) + l_{c2}\cos(\theta_1+\theta_2)\right) \\ m_2 l_{c2} g\cos(\theta_1+\theta_2) \end{bmatrix}$$

with the values of parameters are given in Table 1.

TABLE 1. parameters of the 2-link robot.

Parameters	Values
m_1, m_2	1.5, 1.3 (kg)
l_1, l_2	1, 0.8 (m)
l_{c1}, l_{c2}	0.5, 0.4 (m)
m_1, m_2	1, 0.8 (kgNm^2)

All simulation in this paper is accomplished by employing the MATLAB/Simulink with the sampling time $10^{-3}s$. The desired trajectories of robot are assumed as

$$\theta_d = \begin{bmatrix} 1.2\cos\left(t/7\right) - 0.7 \\ \sin\left(t/6 + \pi/2\right) - 0.4 \end{bmatrix} \tag{38}$$

The robot frictions and disturbances are assumed as

$$F(\dot{\theta}) = \begin{bmatrix} 1.9\cos\left(2\dot{q}_1\right) \\ 1.05\cos\left(\dot{q}_2\right) \end{bmatrix} \tag{39}$$

$$\tau_d = \begin{bmatrix} 2.5\sin(t) + 0.4\cos(\pi t) \\ \cos(t) + 0.6\sin(t/\pi) \end{bmatrix} \tag{40}$$

To validate the property in handling the fault effects, two cases of faults are assumed to impact the robot system. Firstly, simple faults Φ_1 are assumed to be occurred to joint 1 at $T_f = 10s$ and to joint 2 at $T_f = 20s$. Secondly, complex faults Φ_2 are assumed to be occurred to both joints at $T_f = 10s$.

$$\Phi_1 = \begin{bmatrix} -9.7\cos(\pi t/7+\pi/5) \\ 8.2\cos(\pi t/5+\pi/4) \end{bmatrix} \tag{41}$$

$$\Phi_2 = \begin{bmatrix} -3.02\theta_1^2 + \sin(\theta_2) + 6.1\cos(\dot{\theta}_1) + 4.5\dot{\theta}_2 \\ +0.7\sin(2t/\pi) \\ 1.5\theta_1 + 3.2\cos(\theta_2) + 2.3\sin(2\dot{\theta}_1) + 9.2\dot{\theta}_2 \\ +0.5\cos(t/\pi) \end{bmatrix} \tag{42}$$

The selected parameters of the controller and observer methods in the simulations are shown in Table 2.

In the first part of simulation, a comparison of the estimation results between the TOSM observer and the SOSM observer is performed. In Fig. 2 and Fig. 3, the achieved velocity estimation errors when faults Φ_1 and Φ_2 occur, are presented, respectively. The results show that the TOSM observer provides the estimation information with higher accuracy than that of the SOSM observer. According to [52], the SOSM observer needs a lowpass filter to rebuild the estimated signal of the lumped uncertainties and faults. This filtration process causes time delay and estimation errors, that reduce the estimation performance of the SOSM observer. Fortunately, this limitation is removed in the TOSM

TABLE 2. parameters of the controller/observer methods.

Controller/Observer methods	Parameters	Values
TOSM observer	L	9
SMC	c	2
	Δ_d, μ	0.5, 0.01
NTSMC	$\beta_1, \beta_2, \lambda, \alpha$	1.5, 0.4, 0.7, 0.3
	Δ_d, μ	0.5, 0.01
Proposed controller	κ_1, κ_2	0.7, 0.7
	μ_1, μ_2, α	1.2, 1.4, 0.6
	Δ_d, μ	0.5, 0.01

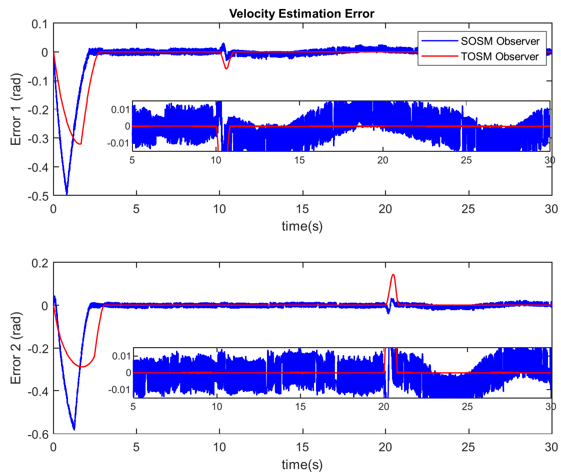

FIGURE 2. The velocity estimation errors are supplied by SOSM observer and TOSM observer at each joint when faults Φ_1 occur.

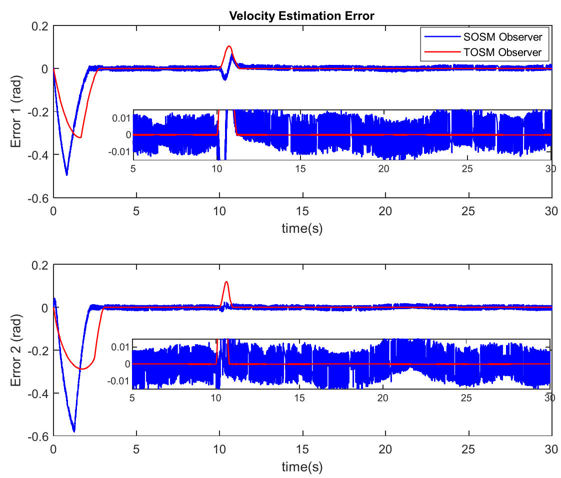

FIGURE 3. The velocity estimation errors are supplied by SOSM observer and TOSM observer at each joint when faults Φ_2 occur.

observer. The estimation results of the lumped uncertainties and faults are presented from Fig. 4 to Fig. 7. In both two cases of faults, the TOSM observer provides higher estimation performance and less chattering than that of the SOSM observer. However, the time response of the TOSM

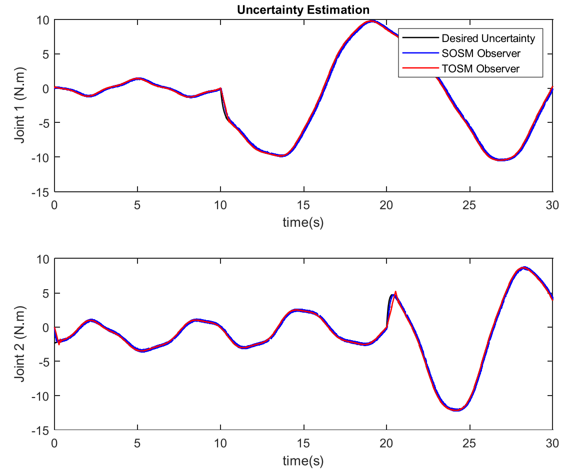

FIGURE 4. The estimation of the lumped uncertainties and faults are supplied by SOSM observer and TOSM observer at each joint when faults Φ_1 occur.

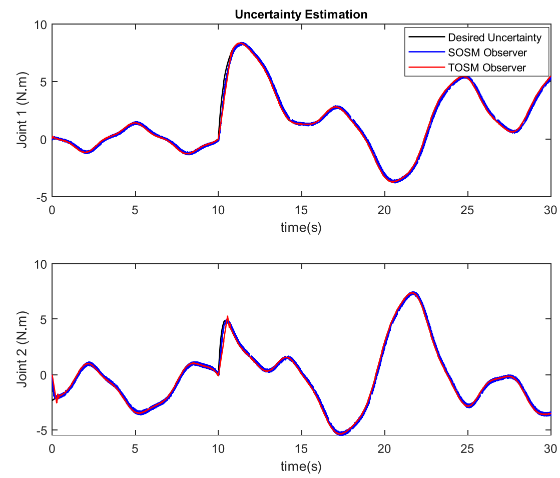

FIGURE 5. The estimation of the lumped uncertainties and faults are supplied by SOSM observer and TOSM observer at each joint when faults Φ_2 occur.

observer is slower. This is also the main limitation of the TOSM observer that needs to improve.

In the second part, a comparison of the proposed FTC algorithm with the control law in (35-37) and the control techniques which are designed based on the conventional SMC (Appendix A) and the NTSMC (Appendix B) is performed to demonstrate its superior control properties. The tracking position and the tracking error at each joint when the simple faults Φ_1 occur are displayed in Fig. 8 and Fig. 10, respectively. As in the results, the real trajectories provided by the proposed FTC method track the desired trajectories with higher accuracy than the FTC methods that are designed based on the conventional SMC and the NTSMC. Compared with the control law in (35-37), the tracking performance that provided by the proposed controller is similar after the convergence process. However, by performing the additional term $\gamma_2 \left|\tilde{x}_1\right|^{1/3} sign\left(\tilde{x}_1\right)$, the proposed FTC method provides

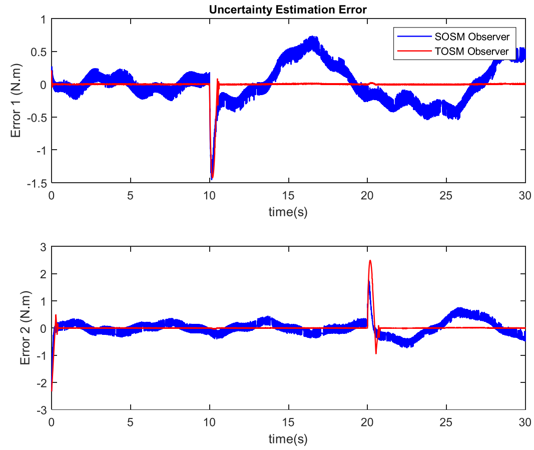

FIGURE 6. The estimation errors of the lumped uncertainties and faults are supplied by SOSM observer and TOSM observer at each joint when faults Φ_1 occur.

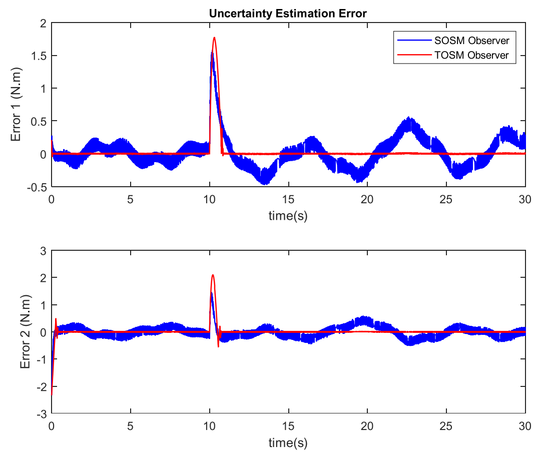

FIGURE 7. The estimation errors of the lumped uncertainties and faults are supplied by SOSM observer and TOSM observer at each joint when faults Φ_2 occur.

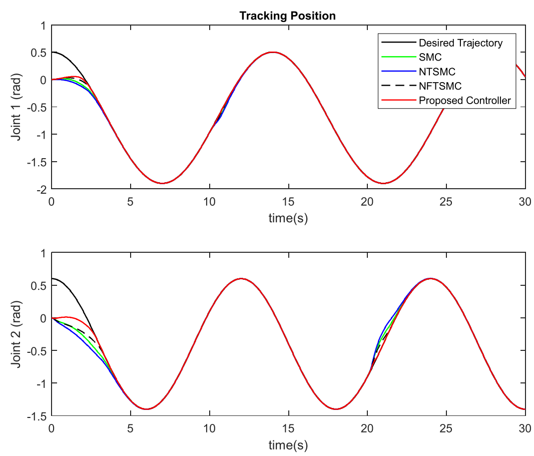

FIGURE 8. Desired trajectories and joint angles are supplied by SMC, NTSMC, NFTSMC, and the proposed controller-observer technique at each joint when faults Φ_1 occur.

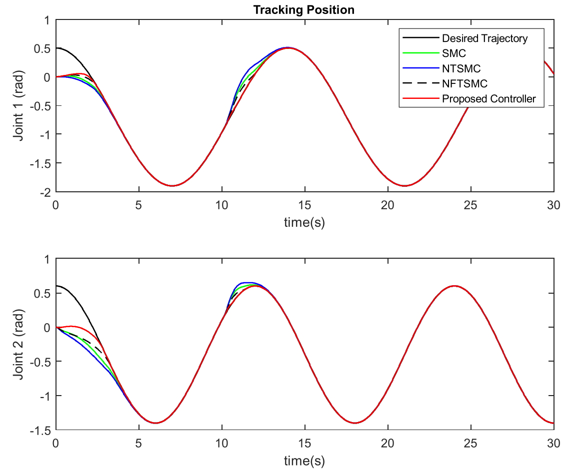

FIGURE 9. Desired trajectories and joint angles are supplied by SMC, NTSMC, NFTSMC, and the proposed controller-observer technique at each joint when faults Φ_2 occur.

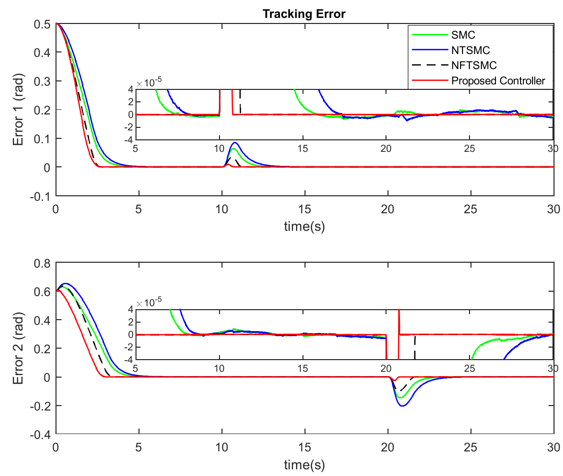

FIGURE 10. Tracking errors are supplied by SMC, NTSMC, NFTSMC, and the proposed controller-observer technique at each joint when faults Φ_1 occur.

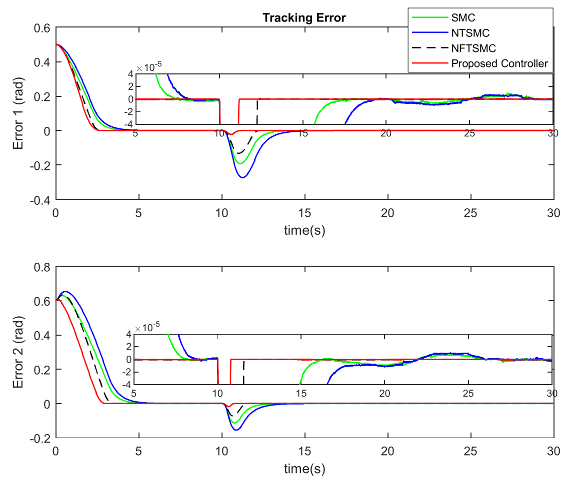

FIGURE 11. Tracking errors are supplied by SMC, NTSMC, NFTSMC, and the proposed controller-observer technique at each joint when faults Φ_2 occur.

faster response at the initial stage and when faults happen. For the case of the complex faults Φ_2, the similar results are obtained and shown in the Fig. 9 and Fig. 11.

The additional term $\gamma_2 \left|\tilde{x}_1\right|^{1/3} sign\left(\tilde{x}_1\right)$ also influences to the convergence of the switching function. As shown in the

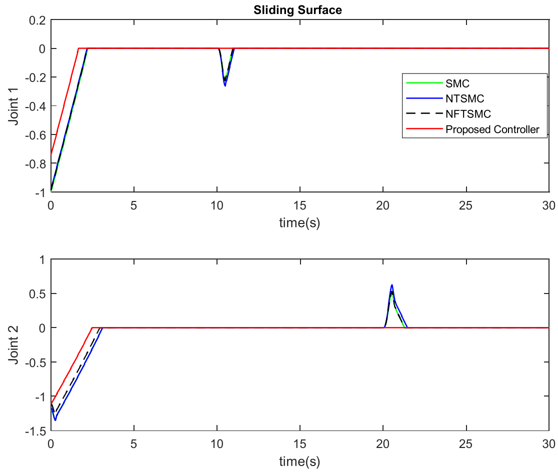

FIGURE 12. Switching functions are supplied by SMC, NTSMC, NFTSMC, and the proposed controller-observer technique at each joint when faults Φ_1 occur.

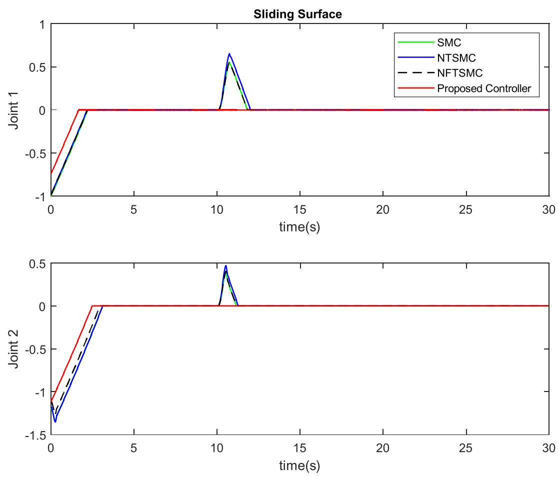

FIGURE 13. Switching functions are supplied by SMC, NTSMC, NFTSMC, and the proposed controller-observer technique at each joint when faults Φ_2 occur.

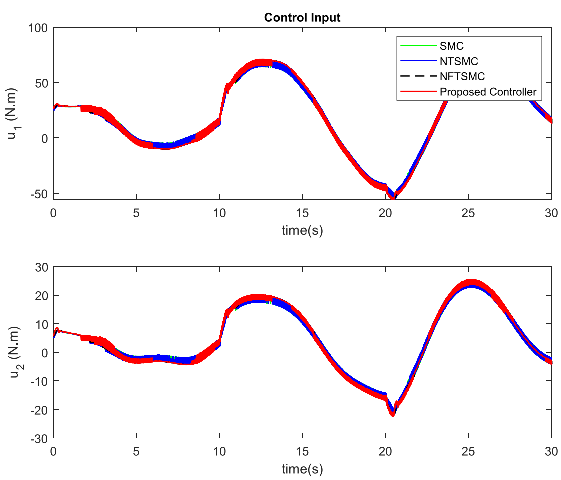

FIGURE 14. Control inputs are supplied by SMC, NTSMC, NFTSMC, and the proposed controller-observer technique at each joint when faults Φ_1 occur.

Fig. 12 and Fig. 13, the switching function of the proposed FTC method converges to zero faster compared with other

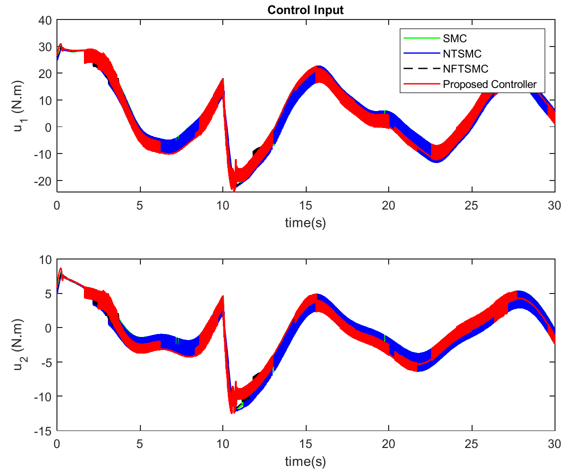

FIGURE 15. Control inputs are supplied by SMC, NTSMC, NFTSMC, and the proposed controller-observer technique at each joint when faults Φ_2 occur.

controllers in both cases of faults. In other words, the sliding motion can be faster reached. In term of the control input torque, the simulation results for both cases of faults of controllers at each joint are presented in Fig. 14 and Fig. 15, respectively. As shown in the figures, by using the proposed FTC algorithm, the chattering phenomenon in the control inputs are reduced due to the compensation of the estimated uncertainties and faults.

VI. CONCLUSION

In this paper, an FTC method using the NFTSMC and the TOSM observer for the robotic manipulator system is proposed. The TOSM observer showed its capability to estimate system velocities; thus, the need of tachometers in the system is eliminated. In addition, the obtained lumped uncertainties and faults are utilized to compensate their effects to the system, thus the tracking performance of the proposed controller-observer method is improved. Moreover, the two stages of time that before and after the convergence time, are carefully analyzed. The proposed FTC method provides advanced control features such as high position tracking precision with fast finite-time convergence, less chattering phenomenon, and robustness against the effects of the lumped uncertainties and faults. The superior control properties of the proposed controller-observer algorithm are fully demonstrated by the simulation results. Further, the proposed method can be applied to the systems that have form of the second-order dynamic systems.

APPENDIX

A. DESIGN OF CONVENTIONAL SMC

With the position and velocity errors are described in (16-17), the conventional switching function based on the TOSM observer is chosen as

$$\hat{s} = \hat{\dot{e}} + ce \tag{43}$$

where c is a positive constant.

The control law is designed as below

$$\tau = -M_0(x_1)\left(\tau_{eq} + \tau_{sw}\right) \tag{44}$$

$$\tau_{eq} = -\ddot{x}_d + \Upsilon(x,t) + \int \gamma_3\, sign(\tilde{x}_1) + c\dot{e} \tag{45}$$

$$\tau_{sw} = (\Delta_d + \mu)\, sign\left(\hat{s}\right) \tag{46}$$

where μ is a small positive constant.

B. DESIGN OF NTSMC

With the position and velocity errors are described in (16-17), the non-singular terminal switching function based on TOSM observer is chosen as in [54]

$$\hat{s} = \hat{\dot{e}} + \beta_1 e + \beta_2 \exp(-\lambda t)\left(e^T e\right)^{-\alpha} e \tag{47}$$

where $\beta_1,\ \beta_2$ are positive constants, $0 < \alpha < 1$, and $\lambda > 0$.

The control law is designed as below

$$\tau = -M_0(x_1)\left(\tau_{eq} + \tau_{sw}\right) \tag{48}$$

$$\tau_{eq} = -\ddot{x}_d + \Upsilon(x,t) + \int \gamma_3\, sign(\tilde{x}_1) + \beta_1 \dot{e} + \beta_2 A \tag{49}$$

$$\tau_{sw} = (\Delta_d + \mu)\, sign\left(\hat{s}\right) \tag{50}$$

where μ is a small positive constant and the term

$$A = [(-\lambda)\exp(-\lambda t)\left(e^T e\right)^{-\alpha} e + (-2\alpha)\exp(-\lambda t)\left(e^T e\right)^{-\alpha-1}\left(e^T \dot{e}\right) e + \exp(-\lambda t)\left(e^T e\right)^{-\alpha}\dot{e}].$$

REFERENCES

[1] M. Van, H.-J. Kang, Y.-S. Suh, and K.-S. Shin, "A robust fault diagnosis and accommodation scheme for robot manipulators," *Int. J. Control, Autom. Syst.*, vol. 11, no. 2, pp. 377–388, Apr. 2013.

[2] M. H. Hamedani, M. Zekri, F. Sheikholeslam, M. Selvaggio, F. Ficuciello, and B. Siciliano, *Fuzzy Sets and Systems*. Amsterdam, The Netherlands: Elsevier, May 2020, doi: 10.1016/j.fss.2020.05.001.

[3] A. T. Vemuri and M. M. Polycarpou, "Neural-network-based robust fault diagnosis in robotic systems," *IEEE Trans. Neural Netw.*, vol. 8, no. 6, pp. 1410–1420, Nov. 1997.

[4] S. N. Huang, K. K. Tan, and T. H. Lee, "Automated fault detection and diagnosis in mechanical systems," *IEEE Trans. Syst., Man, Cybern. C, Appl. Rev.*, vol. 37, no. 6, pp. 1360–1364, Nov. 2007.

[5] Y. Zhang and J. Jiang, "Bibliographical review on reconfigurable fault-tolerant control systems," *Annu. Rev. Control*, vol. 32, no. 2, pp. 229–252, Dec. 2008.

[6] C. Zhang, M.-Z. Dai, P. Dong, H. Leung, and J. Wang, "Fault-tolerant attitude stabilization for spacecraft with low-frequency actuator updates: An integral-type event-triggered approach," *IEEE Trans. Aerosp. Electron. Syst.*, vol. 57, no. 1, pp. 729–737, Feb. 2021.

[7] M. Benosman and K.-Y. Lum, "Passive actuators' fault-tolerant control for affine nonlinear systems," *IEEE Trans. Control Syst. Technol.*, vol. 18, no. 1, pp. 152–163, Jan. 2010.

[8] J. D. Stefanovski, "Passive fault tolerant perfect tracking with additive faults," *Automatica*, vol. 87, pp. 432–436, Jan. 2018.

[9] I. Sadeghzadeh, A. Mehta, A. Chamseddine, and Y. Zhang, "Active fault tolerant control of a quadrotor UAV based on gainscheduled PID control," in *Proc. 25th IEEE Can. Conf. Electr. Comput. Eng. (CCECE)*, Apr. 2012, pp. 1–4.

[10] Q. Shen, C. Yue, C. H. Goh, and D. Wang, "Active fault-tolerant control system design for spacecraft attitude maneuvers with actuator saturation and faults," *IEEE Trans. Ind. Electron.*, vol. 66, no. 5, pp. 3763–3772, May 2019.

[11] B. Zhao and Y. Li, "Local joint information based active fault tolerant control for reconfigurable manipulator," *Nonlinear Dyn.*, vol. 77, no. 3, pp. 859–876, Aug. 2014.

[12] L. A. Castaneda, A. Luviano-Juarez, and I. Chairez, "Robust trajectory tracking of a delta robot through adaptive active disturbance rejection control," *IEEE Trans. Control Syst. Technol.*, vol. 23, no. 4, pp. 1387–1398, Jul. 2015.

[13] H. Wang, W. Bai, and P. X. Liu, "Finite-time adaptive fault-tolerant control for nonlinear systems with multiple faults," *IEEE/CAA J. Automatica Sinica*, vol. 6, no. 6, pp. 1417–1427, Nov. 2019.

[14] F. Luan, J. Na, Y. Huang, and G. Gao, "Adaptive neural network control for robotic manipulators with guaranteed finite-time convergence," *Neurocomputing*, vol. 337, pp. 153–164, Apr. 2019.

[15] W. He, Y. Chen, and Z. Yin, "Adaptive neural network control of an uncertain robot with full-state constraints," *IEEE Trans. Cybern.*, vol. 46, no. 3, pp. 620–629, Mar. 2016.

[16] M. Roopaei and M. Zolghadri Jahromi, "Chattering-free fuzzy sliding mode control in MIMO uncertain systems," *Nonlinear Anal., Theory, Methods Appl.*, vol. 71, no. 10, pp. 4430–4437, Nov. 2009.

[17] S. Ling, H. Wang, and P. X. Liu, "Adaptive fuzzy dynamic surface control of flexible-joint robot systems with input saturation," *IEEE/CAA J. Autom. Sinica*, vol. 6, no. 1, pp. 97–106, Jan. 2019.

[18] M. Van, X. P. Do, and M. Mavrovouniotis, "Self-tuning fuzzy PID-nonsingular fast terminal sliding mode control for robust fault tolerant control of robot manipulators," *ISA Trans.*, vol. 96, pp. 60–68, Jan. 2020.

[19] M. Chen, W. H. Chen, "Sliding mode control for a class of uncertain nonlinear system based on disturbance observer," *Int. J. Adapt. Control Signal Process.*, vol. 24, no. 1, pp. 51–64, 2010.

[20] X.-T. Tran and H.-J. Kang, "Adaptive hybrid high-order terminal sliding mode control of MIMO uncertain nonlinear systems and its application to robot manipulators," *Int. J. Precis. Eng. Manuf.*, vol. 16, no. 2, pp. 255–266, Feb. 2015.

[21] M. Van, "An enhanced robust fault tolerant control based on an adaptive fuzzy PID-nonsingular fast terminal sliding mode control for uncertain nonlinear systems," *IEEE/ASME Trans. Mechatronics*, vol. 23, no. 3, pp. 1362–1371, Jun. 2018.

[22] A. T. Vo and H.-J. Kang, "An adaptive terminal sliding mode control for robot manipulators with non-singular terminal sliding surface variables," *IEEE Access*, vol. 7, pp. 8701–8712, 2019.

[23] V.-C. Nguyen, A.-T. Vo, and H.-J. Kang, "Continuous PID sliding mode control based on neural third order sliding mode observer for robotic manipulators," in *Proc. Int. Conf. Intell. Comput.*, Aug. 2019, pp. 167–178.

[24] A. T. Vo, H.-J. Kang, and V.-C. Nguyen, "An output feedback tracking control based on neural sliding mode and high order sliding mode observer," in *Proc. 10th Int. Conf. Hum. Syst. Interact. (HSI)*, Jul. 2017, pp. 161–165.

[25] V.-C. Nguyen and H.-J. Kang, "A fault tolerant control for robotic manipulators using adaptive non-singular fast terminal sliding mode control based on neural third order sliding mode observer," in *Proc. Int. Conf. Intell. Comput.*, Oct. 2020, pp. 202–212.

[26] Z. Ma, Z. Liu, and P. Huang, "Fractional-order control for uncertain teleoperated cyber-physical system with actuator fault," *IEEE/ASME Trans. Mechatronics*, early access, Nov. 24, 2020, doi: 10.1109/TMECH.2020.3039967.

[27] Y. Wu, X. Yu, and Z. Man, "Terminal sliding mode control design for uncertain dynamic systems," *Syst. Control Lett.*, vol. 34, no. 5, pp. 281–287, Jul. 1998.

[28] M. Zhihong, A. P. Paplinski, and H. R. Wu, "A robust MIMO terminal sliding mode control scheme for rigid robotic manipulators," *IEEE Trans. Autom. Control*, vol. 39, no. 12, pp. 2464–2469, Dec. 1994.

[29] X. Yu and M. Zhihong, "Fast terminal sliding-mode control design for nonlinear dynamical systems," *IEEE Trans. Circuits Syst. I, Fundam. Theory Appl.*, vol. 49, no. 2, pp. 261–264, Aug. 2002.

[30] S. Yu, X. Yu, and R. Stonier, "Continuous finite-time control for robotic manipulators with terminal sliding modes," in *Proc. 6th Int. Conf. Inf. Fusion*, Jul. 2003, pp. 1433–1440.

[31] Y. Feng, X. Yu, and Z. Man, "Non-singular terminal sliding mode control of rigid manipulators," *Automatica*, vol. 38, no. 12, pp. 2159–2167, Dec. 2002.

[32] C.-K. Lin, "Nonsingular terminal sliding mode control of robot manipulators using fuzzy wavelet networks," *IEEE Trans. Fuzzy Syst.*, vol. 14, no. 6, pp. 849–859, Dec. 2006.

[33] S. Sheng-Dong Xu, C.-C. Chen, and Z.-L. Wu, "Study of nonsingular fast terminal sliding-mode fault-tolerant control," *IEEE Trans. Ind. Electron.*, vol. 62, no. 6, pp. 3906–3913, Jun. 2015.
[34] M. Van, S. S. Ge, and H. Ren, "Finite time fault tolerant control for robot manipulators using time delay estimation and continuous nonsingular fast terminal sliding mode control," *IEEE Trans. Cybern.*, vol. 47, no. 7, pp. 1681–1693, Jul. 2017.
[35] A. T. Vo and H.-J. Kang, "An adaptive neural non-singular fast-terminal sliding-mode control for industrial robotic manipulators," *Appl. Sci.*, vol. 8, no. 12, p. 2562, Dec. 2018.
[36] V.-C. Nguyen, A.-T. Vo, and H.-J. Kang, "A non-singular fast terminal sliding mode control based on third-order sliding mode observer for a class of second-order uncertain nonlinear systems and its application to robot manipulators," *IEEE Access*, vol. 8, pp. 78109–78120, 2020.
[37] X. Zhu, H. Zhang, B. Yang, and G. Zhang, "Cloud-based shaft torque estimation for electric vehicle equipped with integrated motor-transmission system," *Mech. Syst. Signal Process.*, vol. 99, pp. 647–660, Jan. 2018.
[38] X. Zhu and W. Li, "Takagi–Sugeno fuzzy model based shaft torque estimation for integrated motor–transmission system," *ISA Trans.*, vol. 93, pp. 14–22, Oct. 2019.
[39] X.-T. Tran, H. Oh, I.-R. Kim, and S. Kim, "Attitude stabilization of flapping micro-air vehicles via an observer-based sliding mode control method," *Aerosp. Sci. Technol.*, vol. 76, pp. 386–393, May 2018.
[40] M. Van, P. Franciosa, and D. Ceglarek, "Fault diagnosis and fault-tolerant control of uncertain robot manipulators using high-order sliding mode," *Math. Problems Eng.*, vol. 2016, pp. 1–14, Sep. 2016.
[41] I. Salgado and I. Chairez, "Adaptive unknown input estimation by sliding modes and differential neural network observer," *IEEE Trans. Neural Netw. Learn. Syst.*, vol. 29, no. 8, pp. 3499–3509, Aug. 2018.
[42] F. Abdollahi, H. A. Talebi, and R. V. Patel, "A stable neural network observer with application to flexible-joint manipulators," in *Proc. ICONIP 9th Int. Conf. Neural Inf. Process. Comput. Intell. E-Age*, vol. 4, Nov. 2002, pp. 1910–1914.
[43] Q. Shen, B. Jiang, P. Shi, and C.-C. Lim, "Novel neural networks-based fault tolerant control scheme with fault alarm," *IEEE Trans. Cybern.*, vol. 44, no. 11, pp. 2190–2201, Nov. 2014.
[44] J. Baek, W. Kwon, B. Kim, and S. Han, "A widely adaptive time-delayed control and its application to robot manipulators," *IEEE Trans. Ind. Electron.*, vol. 66, no. 7, pp. 5332–5342, Jul. 2019.
[45] M. Jin, S. H. Kang, and P. H. Chang, "Robust compliant motion control of robot with nonlinear friction using time-delay estimation," *IEEE Trans. Ind. Electron.*, vol. 55, no. 1, pp. 258–269, Jan. 2008.
[46] F. A. Ortiz-Ricardez, T. Sanchez, and J. A. Moreno, "Smooth Lyapunov function and gain design for a second order differentiator," in *Proc. 54th IEEE Conf. Decis. Control (CDC)*, Dec. 2015, pp. 5402–5407.
[47] Q. Xu, "Continuous integral terminal third-order sliding mode motion control for piezoelectric nanopositioning system," *IEEE/ASME Trans. Mechatronics*, vol. 22, no. 4, pp. 1828–1838, Aug. 2017.
[48] Y. Feng, F. Han, and X. Yu, "Chattering free full-order sliding-mode control," *Automatica*, vol. 50, no. 4, pp. 1310–1314, Apr. 2014.
[49] M. Van, S. Sam Ge, and H. Ren, "Robust fault-tolerant control for a class of second-order nonlinear systems using an adaptive third-order sliding mode control," *IEEE Trans. Syst., Man, Cybern. Syst.*, vol. 47, no. 2, pp. 221–228, Feb. 2017.
[50] X.-T. Tran and H.-J. Kang, "Continuous adaptive finite-time modified function projective lag synchronization of uncertain hyperchaotic systems," *Trans. Inst. Meas. Control*, vol. 40, no. 3, pp. 853–860, Feb. 2018.
[51] A. Levant, "Higher-order sliding modes, differentiation and output-feedback control," *Int. J. Control*, vol. 76, nos. 9–10, pp. 924–941, Jan. 2003.
[52] M. Van, H.-J. Kang, Y.-S. Suh, and K.-S. Shin, "Output feedback tracking control of uncertain robot manipulators via higher-order sliding-mode observer and fuzzy compensator," *J. Mech. Sci. Technol.*, vol. 27, no. 8, pp. 2487–2496, Aug. 2013.
[53] S. P. Bhat and D. S. Bernstein, "Finite-time stability of continuous autonomous systems," *SIAM J. Control Optim.*, vol. 38, no. 3, pp. 751–766, Jan. 2000.
[54] M.-D. Tran and H.-J. Kang, "Nonsingular terminal sliding mode control of uncertain second-order nonlinear systems," *Math. Problems Eng.*, vol. 2015, pp. 1–8, Jan. 2015.

VAN-CUONG NGUYEN received the B.S. degree in electronic and telecommunication engineering from the Danang University of Technology, Danang, Vietnam, in 2014. He is currently pursuing the Ph.D. degree with the School of Electrical Engineering, University of Ulsan, Ulsan, South Korea. His research interests include robot fault diagnosis, fault tolerant control, sliding mode control, and intelligent control.

ANH-TUAN VO received the B.S. degree in electrical engineering from the Danang University of Technology, Danang, Vietnam, in 2008, the M.S. degree in automation from the University of Danang–Danang University of Science and Technology, Danang, in 2013, and the Ph.D. degree in electrical engineering from the Graduate School, University of Ulsan, Ulsan, South Korea, in 2021. He has published more than 20 articles in journals and international conferences. His research interests include intelligent control, sliding mode control and its application, and fault-tolerant control.

HEE-JUN KANG received the B.S. degree in mechanical engineering from Seoul National University, South Korea, in 1985, and the M.S. and Ph.D. degrees in mechanical engineering from The University of Texas at Austin, USA, in 1988 and 1991, respectively. Since March 1992, he has been a Professor of electrical engineering with the University of Ulsan. His current research interests include sensor-based robotic application, robot calibration, haptics, robot fault diagnosis, and mechanism analysis.